



國立臺灣大學生命科學學院
學士班學生論文

Department of Life Science
College of Life Sciences
National Taiwan University
Bachelor Degree Thesis

探討腺苷酸甲基化辨識蛋白 *DjYTHDC1* 與 *DjYTHDF* 參
與在渦蟲再生和神經發育之功能

Study the role of *DjYTHDC1* and *DjYTHDF* in planarian
regeneration and development of nervous system

李淑芬

Stephanie Evelyn

指導教授：朱家瑩 博士

Advisor: Chia-Ying Chu, Ph.D.

中華民國 111 年 4 月

April 2022



國立臺灣大學學士班學生論文
口試委員會審定書

探討腺苷酸甲基化辨識蛋白 *DjYTHDC1* 與
DjYTHDF 參與在渦蟲再生和神經發育之功能
**Study the role of *DjYTHDC1* and *DjYTHDF* in
planarian regeneration and development of nervous
system**

本論文係李淑芬君 (B07B01044) 在國立臺灣大學生命科學學系完成之學士班學生論文，於民國 111 年 04 月 01 日承下列考試委員審查通過及口試及格，特此證明

口試委員(3位)：

朱家蓉

(簽名)

陳文國 (指導教授)

周銘羽

鄧豐翹

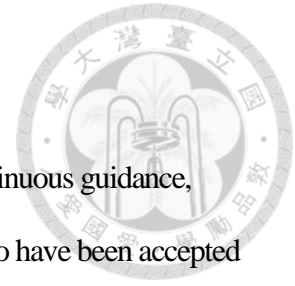
系主任：

黃偉邦

(簽名)

(是否須簽章依各院系規定)

Acknowledgements



Firstly, I would like to thank my advisor dr. Chu Chia-Ying for the continuous guidance, discussions and support during the completion of this thesis. I am very grateful to have been accepted into her lab despite my lack of previous research experience. It has been a great opportunity to learn and train with her. She was also a great source of support in times when I doubted my ability, and a great source of guidance in the completion of this thesis. Second, I would like to thank dr. Kuo Dian-Han for taking the time to be one of the thesis defense committee members, and the constant willingness to provide guidance and assistance. Third, I would like to thank dr. Chen Shih-Kuo for the taking the time to be one of the thesis defense committee members, as well as the ideas given during the discussion. I would also like to thank dr. Zhou Ming-Yi for the ideas and discussions during seminar, the guidance provided during the preparation for seminar presentation, and taking the time to be one of the thesis defense committee members.

I would like to thank all members of Chu lab for the guidance and support during the 2-year period I was in the lab. Thank you to my seniors Xu Jing-Jie and Xu Yan-Jie for the guidance, discussions and the knowledge given, and were always willing to aid since the beginning to now. I am also grateful for their care and support any time I experienced difficulties and being patient while teaching me. Thank you to seniors Chu Yi-Ning and Han Tian-Heng for the discussions and guidance while learning new techniques, and the helpful know-hows that were passed down. I would also like to thank senior Shih Jia-Yu, Lin Heng-Yi and Zheng Yi-Shan for the helpful advice and support. I would like to especially thank my partner in the lab Su Yi-Jia, who I have greatly depended on for mental support and whom I have had many discussions with.

摘要

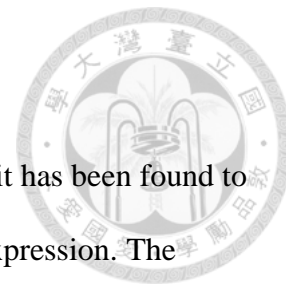


腺苷酸甲基化修飾 (m^6A) 是真核生物中重要的轉錄後修飾方式之一，此修飾能調控 RNA 的穩定、剪接、運輸、及轉譯，因此參與疾病發生以及動物的發育等過程。細胞中存在 m^6A 修飾的偵測蛋白，透過辨識 m^6A 修飾的 RNA 後引導其他相關蛋白的結合，進而產生後續作用。例如：YTHDF2 結合到具有 m^6A 修飾的 RNA 上後會引導 CCR4-NOT 蛋白和 RNA 的結合，導致 RNA 降解的速率增加。過去研究多專注於對脊椎動物的 m^6A 機制和功能，但對無脊椎動物或具有再生能力的動物中的 m^6A 功能則仍未有足夠的研究證據。由於渦蟲具有很強的再生能力，能透過體內散布的成體幹細胞 (Neoblast) 在斷裂後 7-14 天內就再生為完整的個體，修補失去的各種組織，但對於後轉錄調控參與再生過程的詳細機制未有深入瞭解，因此本研究利用渦蟲作為研究對象，探討 m^6A 修飾的偵測蛋白 DjYTHDC1 以及 DjYTHDF 在再生過程中及神經系統發育的角色。

本研究發現渦蟲體內的 *DjYTHDC1* 大量表現於神經系統而 *DjYTHDF* 表現於成體幹細胞 (Neoblast) 中。以 RNAi 的方式降低 *DjYTHDC1* 或 *DjYTHDF* 的表現後，導致渦蟲體內 cNeoblast 的數量減少以及降低負趨光性反應。如果在再生的過程中持續降低 *DjYTHDC1* 或 *DjYTHDF* 的表現時，出現眼睛再生延遲、芽胞再生組織 (blastema) 變小以及神經元異常分佈的結果。本研究結果證明了 m^6A 偵測蛋白 DjYTHDC1 及 DjYTHDF 對與再生及神經系統的發育和功能具有重要性，提供未來探討 m^6A 偵測蛋白如何影響分裂分化，以及在神經系統參與的途徑的可能研究方向。

關鍵字：核糖核酸甲基辨識蛋白、*DjYTHDC1*、*DjYTHDF*、再生、神經系統發育、渦蟲

Abstract

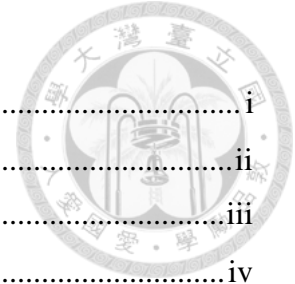


m⁶A is one of the most abundant types of RNA modification, and it has been found to be involved in various steps of post-transcriptional regulation of gene expression. The functions of m⁶A in the cell is mediated by reader proteins that bind specifically to m⁶A modification in the RNA. Although the role of m⁶A in vertebrates have been largely studied, its role in invertebrates and regeneration is scarcely understood. Since planarian have robust regenerative ability that relies on its adult stem cells called neoblasts, it has been used as a suitable organism for studying regeneration. Therefore, this research aims to study the function m⁶A readers in regeneration and its effects on the development of nervous system.

Through this study, we found that m⁶A reader proteins in planarian, *DjYTHDC1* was expressed mainly in the nervous system, whereas *DjYTHDF* was expressed mainly in the neoblasts. Depletion of either reader proteins reduced the number of cNeoblasts and altered the number of progeny cells, as well as reduce negative phototaxis responses in intact worms. During regeneration, depletion of either reader proteins caused the delay in eye regeneration, and decreased the blastema size, as well as disrupting the distribution pattern of several neural subtypes. Taken together, I found that *DjYTHDC1* and *DjYTHDF* play roles in the proper regeneration of the eye and neural subtypes, as well as in regulating negative phototaxis behavior, suggesting the essential role of m⁶A modification in planarian nervous system.

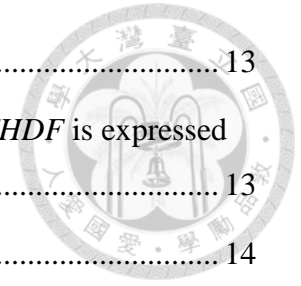
Keywords: M⁶A reader proteins, *DjYTHDC1*, *DjYTHDF*, regeneration, Nervous system development, planarian

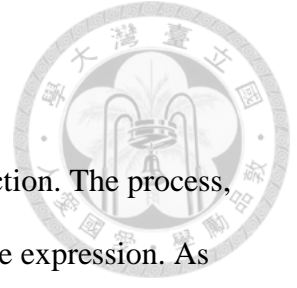
Table of contents



口試委員審定書	i
Acknowledgements	ii
摘要	iii
Abstract.....	iv
Table of contents	v
1. Introduction	1
1.1. RNA editing and RNA modification	1
1.2. m ⁶ A RNA modification	2
1.3. m ⁶ A reader proteins and its role in mediating m ⁶ A function.....	3
1.4. Planarian regeneration	4
1.5. The nervous system of planarians.....	5
1.6. Specific aims.....	6
2. Material and Method	7
2.1. <i>Dugesia japonica</i> culture	7
2.2. TA cloning	7
2.3. Phylogenetic analysis.....	8
2.4. RNA extraction and reverse transcription PCR (RT-PCR)	9
2.5. Quantitative polymerization chain reaction (qPCR).....	9
2.6. RNA interference (RNAi).....	9
2.7. Fluorescence activated cell sorting (FACS)	10
2.8. Whole-mount in situ hybridization (WISH)	10
2.9. Immunofluorescence staining (IF).....	10
2.10. Phototaxis assay	11
2.11. Quantification of eye regeneration delay.....	11
2.12. Quantification of blastema size.....	12
3. Results.....	13

3.1.	Identification of m ⁶ A reader genes in planarian	13
3.2.	<i>DjYTHDC1</i> is highly expressed in the brain region while <i>DjYTHDF</i> is expressed diffused throughout the parenchyma	13
3.3.	<i>DjYTHDC1</i> and <i>DjYTHDF</i> are expressed in the neoblast	14
3.4.	<i>DjYTHDC1</i> and <i>DjYTHDF</i> depletion in intact planarian shows evident effects on neoblast and neural genes	16
3.5.	<i>DjYTHDC1</i> and <i>DjYTHDF</i> are required for expression of neuron subtypes marker genes and regulates planarian behavior	17
3.6.	Depletion of m ⁶ A readers affects development of several neuron subtypes	19
4.	Discussion	23
5.	References	26
6.	Figures	29





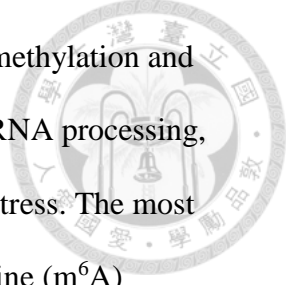
1. Introduction

Genes are the basic blueprint of how an organism appears and function. The process, which carries traits encoded within genes into a phenotype, is called gene expression. As the central dogma states, gene expression includes two steps: transcription is the process where cells use DNA as the template to synthesize RNAs, and translation is the process of generating polypeptide using RNA as the template in ribosomes. Interestingly, the same genes in different organs or tissues might be turned on under different circumstances, and the difference in gene regulation is able to cause different phenotypes (Roscito *et al.*, 2018).

In addition to the transcriptional control, regulation of gene expression largely depends on post-transcriptional modifications of mRNA and other RNA to regulate its level in the cell. As the need for protein product of a certain gene changes, mRNA can be degraded or produced accordingly, this results in changing the levels of RNA in the cell (Roundtree *et al.*, 2017).

1.1. RNA editing and RNA modification

One type of post-transcriptional regulation at RNA level is RNA modification, which can be done by adding or removing chemical groups from RNA or by changing the secondary structure of RNA. For example, the A-to-I RNA editing is the deamination on adenine that will change Adenine into Inosine. Since Inosine could base-pair with cytidine, it acts as a guanosine in the codon recognition, thus generates extra stop codon or changes amino acid sequences for coding region. This change of amino acid sequence will result in either non-functional protein product, or the premature stop codon that most likely triggers RNA degradation (Nishikura, 2016). Aside from deamination, other modification such as



methylation and acetylation are also observed in RNA molecules. Both methylation and acetylation on RNAs are known for its involvement in regulating pre-mRNA processing, mRNA metabolism, and initiation of cap independent translation under stress. The most abundant type of modification in eukaryotic mRNA is N⁶-Methyladenosine (m⁶A) modification (Roundtree *et al.*, 2017).

1.2. m⁶A RNA modification

m⁶A is the methylation of the nitrogen atom of adenosine at the position 6 of nitrogenous base. Previous studies have found that m⁶A is involved in regulating splicing, stability, turnover, nuclear export and mediating the cap-independent translation of mRNA and ncRNA (Liu and Jia, 2014; Meyer *et al.*, 2015). In addition to its involvement in regulating the half-life of mRNAs, it was also found to be enriched to the nervous system and regulate the neuronal function and sex determination in *Drosophila* (Lence *et al.*, 2016). Recently, it has been found that the downregulation of m⁶A modifications has an important role in apoptosis of dopaminergic neurons in mammals (Chen *et al.*, 2019). One study found that reduction in m⁶A modification results in the induced expression of NMDA receptor 1, as well as the increased oxidative stress and Ca²⁺ influx.

Researchers have found that the dynamics of m⁶A modification are dependent on certain proteins able to encode (writers), decode (readers) and remove (erasers) the methylation on adenosine (Figure 1.1.) (Lewis *et al.*, 2017). Since the discovery of the proteins in control of the dynamics of m⁶A modifications, functions of these proteins in different organisms have been studied in detail.

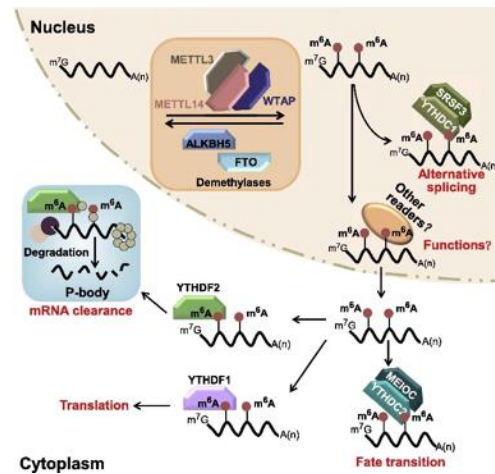


Figure 1.1. The proteins involved in regulating m⁶A modification

1.3. m⁶A reader proteins and its role in mediating m⁶A function

The most-well studied of the m⁶A readers are proteins containing YTH domain. YTH domain is predicted to function as an RNA binding domain based on its homology with RRM (RNA recognition motif). In vertebrates, YTH-domain containing proteins can be classified into three types, YTH-domain containing protein family (YTHDF), YTH-domain containing protein 1 (YTHDC1) and YTH-domain containing protein 2 (YTHDC2) (Patil *et al.*, 2018).

Although their role and function are still largely unknown, various studies have shown that YTH-domain containing proteins functions in regulating mRNA levels. The three paralogs of YTHDF, namely YTHDF1, YTHDF2, and YTHDF3, share similar amino acid sequences throughout their entire length and are found to bind predominantly in the cytoplasmic mRNAs (Patil *et al.*, 2018). YTHDF1 and 2 are found to be responsible for RNA stability, YTHDF1 is found to have a role in regulating translation (Wang *et al.*, 2015), while YTHDF2 is found to affect mRNA decay by recruiting of CCR4-NOT deadenylase complex, thereby promoting deadenylation of mRNA. Interestingly, YTHDF3

is found to have a combined function of translational enhancement and mRNA degradation (Li *et al.*, 2017; Shi *et al.*, 2017). The YTH-domain containing protein YTHDC1 have binding sites that nearly completely overlaps with m⁶A sites in nuclear RNA and is found to play a role in alternative splicing.

In vertebrates, the role of YTHDF2 in development has been well studied. In mice, research has discovered that YTHDF2 is involved in the neural development of mouse embryo, and knockdown of the m⁶A reader results in lethality caused by compromised neural development (Li *et al.*, 2018). In *Drosophila*, both YTHDF and YTHDC1 has been shown to be involved in brain functioning such as learning and memory as well as flight behavior and locomotion (Kan *et al.*, 2021; Lence *et al.*, 2016). In zebrafish, a study shows that knockdown of YTHDF2 would affect maternal to zygotic transition by impeding zygotic genome activation (Zhao *et al.*, 2017). However, there has been no conclusive report of the role of m⁶A in other invertebrates and in animals with regeneration ability (Lence *et al.*, 2017). One of the model organisms in which to study regeneration is planarian.

1.4. Planarian regeneration

Two species of planarian, *Schmidtea mediterranea* (smed) and *Dugesia japonica* (Dj), are commonly used as the model organism in modern biology. Contrary to the limited regenerative ability of vertebrates and some invertebrates, planarians could regenerate whole individuals after injury or fragmentation. Planarian has a robust regenerative ability that is able to grow whole individuals from 1/279th of the intact worm in just seven days. Planarians are able to regenerate all of their body parts including complete heads. The

robust regenerative ability of planarian depends on the proliferation and differentiation of adult stem cells called neoblasts.



Neoblasts are pluripotent adult somatic stem cells that are distributed throughout the planarian body. Neoblasts are the cells with proliferative ability and express genes regulating the maintenance of pluripotency. Recent studies have found that neoblasts can be further classified into different stemness states, based on the differential expression of marker genes in single cell transcriptome data. The cells in the most pluripotent cells are named cNeoblasts, which express both *piwi-A* and *tdg-1* (Zeng *et al.*, 2018).

After injury, wound sites will induce neoblast proliferation, which will result in the forming of newly grown tissue, called blastema. It can be expected that such robust regenerating ability would need accurate regulation of regenerating and differentiation genes in order to spatially and temporally direct regeneration (Rink, 2013).

1.5. The nervous system of planarians

In contrast to limited neurogenesis in vertebrates and other organism, planarians are able to regenerate the complete nervous system. The nervous system of a planarian consists of a cephalic ganglion, ventral nerve cord and lateral branches. In addition, studies have found that the nervous system of planarian includes five different neuron subtypes (Figure 1.2.), including GABAergic, dopaminergic, cholinergic, serotonergic and octopaminergic. Different types of neurons contribute to regulating various behaviors such as phototaxis, thermotaxis as well as drug-induced locomotion (Ross *et al.*, 2017).

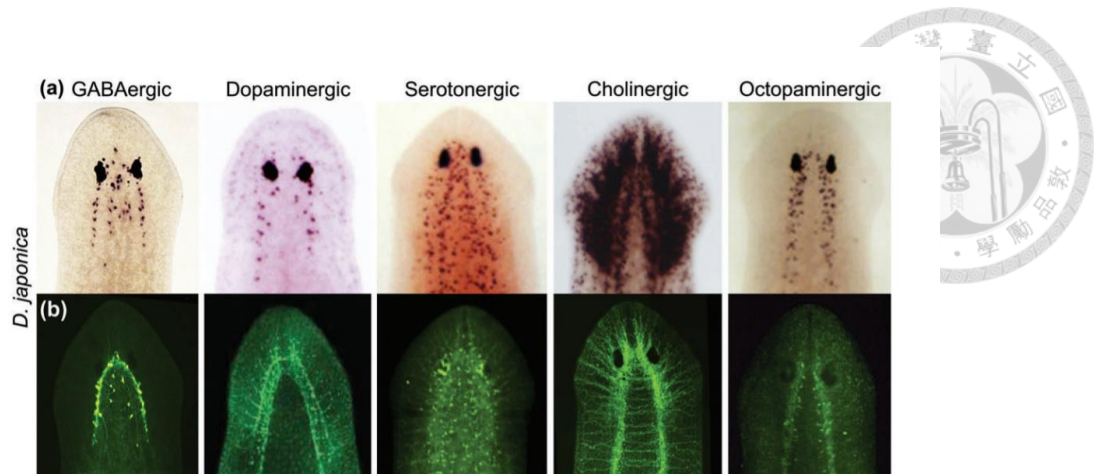


Figure 1.2. The neuron subtypes of planarian

1.6. Specific aims

Previous studies showed m⁶A readers were important in animal development. However, it is unclear whether planarian express m⁶A reader homologs and whether m⁶A modification participates in regulating regeneration. Since planarian exhibits robust regenerative ability paired with its ability to regenerate the nervous system rapidly, it has become a very interesting model organism in which to study the development of the nervous system. Therefore, my study aims to answer the following questions:

1. What is the role of m⁶A reader proteins in planarian regeneration?
2. What is the role of m⁶A reader proteins in the nervous system and neuronal development?



2. Material and Method

2.1. *Dugesia japonica* culture

The *Dugesia japonica* used in this research is captured in yilan county of Taiwan.

Planarians reproduce both asexually and sexually, which varies depending on the environment and maturity of its reproductive organs. The planarians used in this research are cultured in aerated water and reproduce asexually, they are fed chicken liver once every 4 days.

2.2. TA cloning

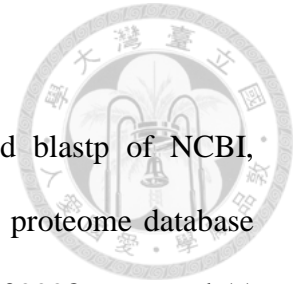
TA cloning is done to isolate and make multiple copies of a gene of interest for later use in a research. The primers used in this research are listed in Table 1. The isolated DNA sequence is inserted into a TA vector, and it is transformed into an LB plate with Ampicillin antibiotic as the selection marker for recombinant bacteria. In addition, X-gal and IPTG are added for blue and white selection for recombinant bacteria. After selection, the colony is amplified in liquid LB medium with ampicillin antibiotic and sequenced.

Table 1. Primers used in this research

Gene name	Primer sequence	Amplicon Length
<i>DjYTHDF_F</i>	5'-GTCATGAACTCAAATAAAAAGT-3'	1040
<i>DjYTHDF_R</i>	5'-CATGAACTCAAATAAAAAGT-3'	
<i>DjYTHDC1_F</i>	5'-CTTAAATGGTTGAAACTGA-3'	920
<i>DjYTHDC1_R</i>	5'-GGAATAAACAATTTCCATAAT-3'	

2.3. Phylogenetic analysis

The sequences used for alignment was found using web-based blastp of NCBI, sequences of YTH proteins for *Euglena gracilis* were taken from the proteome database (<http://proteomecentral.proteomexchange.org/cgi/GetDataset?ID=PXD009998>, accessed 11 April 2022). The outgroup was chosen by referring to a previous phylogenetic analysis of the YTH domain proteins (Liu et al., 2022). The sequence alignment was made using CLC sequence viewer with default settings, the YTH domain of each protein was identified using batch mode of NCBI conserved domain search service. The evolutionary history was inferred by using the Maximum Likelihood method and Le_Gascuel_2008 model. The bootstrap consensus tree inferred from 1000 replicates is taken to represent the evolutionary history of the taxa analyzed. Branches corresponding to partitions reproduced in less than 50% bootstrap replicates are collapsed. The percentage of replicate trees in which the associated taxa clustered together in the bootstrap test 1000 replicates) are shown above the branches. Initial tree(s) for the heuristic search were obtained by applying the Neighbor-Joining method to a matrix of pairwise distances estimated using the JTT model. A discrete Gamma distribution was used to model evolutionary rate differences among sites (2 categories (+G, parameter = 2.7854)). This analysis involved 16 amino acid sequences. All positions with less than 95% site coverage were eliminated, i.e., fewer than 5% alignment gaps, missing data, and ambiguous bases were allowed at any position (partial deletion option). There was a total of 179 positions in the final dataset. Evolutionary analyses were conducted in MEGA11.



2.4. RNA extraction and reverse transcription PCR (RT-PCR)

The worms used for RNA extraction are starved for a week before the extraction is performed. After the worms are starved, 5-6 worms are fixed in Trizol. The worms are then homogenized using a homogenizer and put on ice before proceeding. Chloroform is added in a 1:50 ratio to the total trizol volume and mixed thoroughly before being centrifuged in 4°C, with centrifugation speed 12000g. The transparent layer is then moved into a new microcentrifuge tube and isopropanol is added to aid precipitation of RNA. It is then put into -20°C for 1 hour or more, and centrifuged again in 4°C, with centrifugation speed 12000g. The RNA is washed and purified with the addition of 75% Ethanol before it is air-dried. The concentration is then immediately measured using a spectrophotometer.

Reverse transcription is done immediately after RNA extraction for all RNA samples. The reaction is done using random hexamer and SS3RT enzyme.

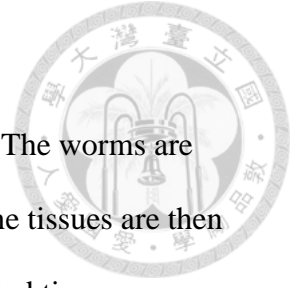
2.5. Quantitative polymerization chain reaction (qPCR)

qPCR is done by using SYBR green mix, with primers designed to be located at introns more than 100bp in length. The experiment is done with Tubulin as loading control and no-RT as a quality control for possible DNA contaminations.

2.6. RNA interference (RNAi)

RNA interference by feeding is done by feeding liver mixed with 4000ng dsRNA and food coloring. The worms are fed once every 4 days for 4 weeks and starved for 4 days before being fixed.

RNA interference by soaking is done by soaking amputated worms in 13µl planarian water mixed with 4000ng dsRNA, in 18°C incubator for 1-3hr once every 4 days until the required time point.



2.7. Fluorescence activated cell sorting (FACS)

The planarians used are starved for 7 days before the experiments. The worms are then cut into small pieces and transferred into a microcentrifuge tube. The tissues are then trypsinized and centrifuged to collect the cells. To filter out any undigested tissues, we applied the solution on 40 and 20 μm filter membranes. The cells are then stained with Hoescht blue and Calcein AM for around 2 hours before it is analyzed using a cell sorter.

2.8. Whole-mount in situ hybridization (WISH)

Whole-mount in situ hybridization used in this research is based on the procedure described (Pearson *et al.*, 2009). The worms are starved for 7 days for wild type worms, and 4 days for RNAi worms. First, they are NAC treated to remove the mucus and fixed with 4% formaldehyde in PBS. The worms are then treated with reduction solution in 37°C, dehydrated using methanol and bleached with H_2O_2 under direct light overnight.

The next day, the worms are rehydrated and treated with proteinase K to help with riboprobe permeabilization. It is then incubated with riboprobe for 18 hours, then washed with prehybe solution and different concentrations of SSC solutions. After several washes, it is then incubated with blocking solution and antibody overnight. The antibody is washed with MABT and developed using NBT and BCIP, then washed with ethanol to reduce background. The specimens are then preserved with 80% glycerol in 4°C.

2.9. Immunofluorescence staining (IF)

Immunofluorescence staining is performed based on the procedure described (Forsthoefel *et al.*, 2018). We utilized NAC to remove the mucus, followed by fixing using formaldehyde and H_2O_2 bleaching. We did not perform reduction and proteinase treatment

for all immunofluorescence staining. The worms are then washed using PBSTx and incubated with the primary antibody overnight. The next day the worms are washed for 6-8 hours and incubated with the secondary antibody overnight. After incubation, the worms are washed with PBSTx and stained with Hoescht blue before it is preserved in 80% glycerol and visualized.

2.10. Phototaxis assay

Phototaxis assay as performed as described (Paskin *et al.*, 2014) with few modifications. The container used for the test was a rectangular shaped box with dimensions 12 cm x 3.5 cm x 3 cm. The container was placed on a white cardboard that divided the container into 4 equal quadrants which are labeled Q1-Q4. A light source (white light) is placed parallel to the container at Q1. The container is filled to a depth of 0.5cm with planarian water for each trial. The planarian is placed in Q1 and allowed to adapt to the new environment for 10 minutes in the dark before each trial. The light is switched on for 2 minutes, and at the end the position of the worms was photographed and recorded. The experiment is conducted in ambient lighting, and the trial is repeated 5 times with 10 minutes rest in between each trial.

2.11. Quantification of eye regeneration delay

The worms are amputated and photographed every day starting from the time of amputation. The worms are observed for 10 days and the condition of eye regeneration is recorded. The standard for the eyespot is that it is bigger than normal pigments, and that it is visible when viewed from the ventral side. The worms are considered to have grown both eyespots when the eyespot grown has similar sizes and are located at the middle of

the head. They are considered to have grown asymmetrical eyes when either one of the eyespots seem to be smaller in size in comparison to the other. Recordings of the eyespot regeneration are calculated as the percentage of worms regenerating either both eyespots, asymmetrical eyespots, one eyespot or no eyespots over the total amount of worms.

During regeneration, the intersection between the nerve from photoreceptor and the optic chiasm will move further away from the two eyecups. Therefore, it can also be used to quantify the delay in regeneration. The immunostaining of planarian with anti-arrestin antibody was performed to visualize the optic chiasm and was analyzed using ImageJ. In the IF images as shown in Figure 12, I defined B as the point where the photoreceptor nerve intersects with the optic chiasm. A vertical line extend from point B is perpendicular to the line connecting the anterior-most side of the two eyecups and cross at point A. The length of optical nerve of each photoreceptor was defined as the distance between point A and B. This is then normalized to the total distance between the two eyecups.

2.12. Quantification of blastema size

The worms are photographed at 3 dpa and the image is then analyzed using ImageJ. In this research, the size of the blastema is considered to be the area of the blastema as measured from the edge of the wound site to the tip of the blastema.



3. Results

3.1. Identification of m⁶A reader genes in planarian

To study the function of m⁶A readers in planarian, I first identified its sequence and confirmed its conservation with the m⁶A reader homologs obtained from other well-studied species. To do this, I used BLAST to find out the sequences of m⁶A readers from the planarian (*Dugesia japonica*) transcriptome database in our lab. Through this process I found two m⁶A readers in the planarian with highly conserved sequences with other well-researched organisms. The first sequence found has high similarity to the YTHDC1 protein, therefore I named it as *DjYTHDC1* (Figure 1A). The second sequence found has high similarity to the YTHDF family proteins; therefore, I named it as *DjYTHDF* (Figure 1B).

From alignment of the predicted YTH domain of the protein sequences of *DjYTHDC1* and *DjYTHDF*, we observed that it has a high similarity to those found in other organisms. To further confirm its evolutionary relationship, I used MEGA to construct a phylogenetic tree (Figure 1C). Through this phylogenetic tree, it can be seen that *DjYTHDC1* and *DjYTHDF* can each be grouped with YTHDC1 and YTHDF from well-studied organisms, therefore proving that the sequences we found are indeed homologues of YTHDC1 and YTHDF in other organisms.

3.2. *DjYTHDC1* is highly expressed in the brain region while *DjYTHDF* is expressed diffused throughout the parenchyma

Since *DjYTHDC1* and *DjYTHDF* are found in the transcriptome of planarian, I am curious to know where in the planarian the readers are expressed, as this might shed light on the function of these readers in the planarian. To analyze the expression pattern of

DjYTHDC1 and *DjYTHDF* in intact planarian, I performed Whole-mount in situ hybridization (WISH). WISH of *DjYTHDC1* and *DjYTHDF* are performed using digoxigenin-labeled antisense RNA probe, with sense probes as control. The RNA probes would attach onto the RNA of interest and would stain a dark blue color due to the digoxigenin labeling.

The resulting staining shows no hybridization of sense probes while antisense probes for *DjYTHDC1*, were found to be enriched in the cephalic ganglia of the planarian, with some expression in the parenchyma. Antisense probes for *DjYTHDF* are found to be expressed diffused throughout the parenchyma of the planarian (Figure 2). The pattern of expression in the parenchyma is similar to the distribution of *Djpiwi-A*, a neoblast marker. Therefore, I hypothesized that *DjYTHDC1* and *DjYTHDF* were both expressed in the neoblasts.

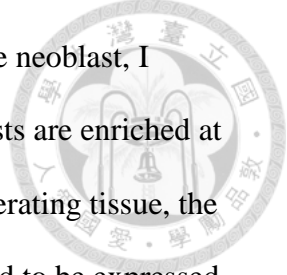
3.3. *DjYTHDC1* and *DjYTHDF* are expressed in the neoblast

To precisely pinpoint the cell fraction that these m⁶A readers are localized to, I did FACS to sort out various types of planarian cells and then extracted the total RNA from each group of cells to further analyze the expression of each m⁶A reader by RT-qPCR (Figure 3A). Cells of different groups were determined by fluorescence signals of Hoescht blue and Hoescht red (Figure 3B). Through Hoescht blue and red fluorescence gating, X1 cells are defined to be mostly consisted of neoblast and proliferating cells, X2 fraction are thought to mostly consist of early progeny cells that are more differentiated than neoblasts but still retain some proliferation ability, and Xins are cells that are insensitive to irradiation and is predicted to consist mostly of differentiated cells. Analysis of the cell fractions from intact worms shows that *DjYTHDC1* is highly expressed throughout all fractions in

decapitated worm sample. On the other hand, *DjYTHDF* is highly expressed in X1 fraction (Figure 3C).

From previous analysis of WISH and FACS of *DjYTHDC1* and *DjYTHDF*, it is possible that both readers may be localized to the neoblasts. Previous research has found that by irradiating planarian with a high dosage, the neoblasts in its body could be eliminated. If the readers were indeed expressed in the neoblast of a planarian, I would expect the level of both readers to be greatly reduced with irradiation. To test this hypothesis, I performed WISH and qPCR of both readers in irradiated worms. Previous irradiation studies claim that the irradiated worms would experience significant expression reduction of the neoblast-specific gene, *Djpiwi-A*, at 2- and 4-days post-irradiation. Therefore, I utilized these two time points to analyze the expression pattern of the readers in irradiated worms.

In the WISH staining result, it can be observed that the irradiated worms experienced some loss in *DjYTHDC1* expression especially near the tail region at 2 dpi. At 4 dpi, it can be observed that the expression in the parenchyma was almost completely removed, with a persistent expression at the cephalic ganglia (Figure 4A). In *DjYTHDF* stained worms, I also observed a reduction in the expression around the parenchyma (Figure 4B). RT-qPCR analysis of the irradiated worms shows highly reduced *Djpiwi-A* expression in both 2dpi and 4dpi worms, this indicates that the neoblasts can be eliminated by irradiation. It can also be observed that there is a reduction in expression level of *DjYTHDC1* and *DjYTHDF* at 2 and 4 dpi (Figure 4C), although the level of both readers was not decreased in proportion to the decrease in *Djpiwi-A*. This result showed that some cells expressing *DjYTHDC1* and *DjYTHDF* are neoblasts.



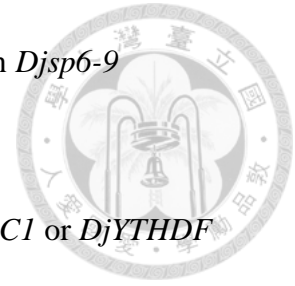
To further validate localization of *DjYTHDC1* and *DjYTHDF* in the neoblast, I performed WISH of each gene in regenerating worms, where the neoblasts are enriched at the blastema. *DjYTHDC1* is found to be highly expressed near the regenerating tissue, the blastema, at day 2 of regeneration, and at day 5 of regeneration it is found to be expressed in the newly regenerated brain (Figure 5A), while *DjYTHDF* is found to be highly expressed near the blastema at day 2 and 5 of regeneration (Figure 5B).

3.4. *DjYTHDC1* and *DjYTHDF* depletion in intact planarian shows evident effects on neoblast and neural genes

So far, I have characterized the expression of *DjYTHDC1* and *DjYTHDF* both in intact and regenerating planarian. The next step would be to characterize its function in planarian. To do this, I performed RNAi by feeding of double-stranded RNA for 4 weeks to specifically knockdown *DjYTHDC1* and *DjYTHDF*. Since *DjYTHDC1* and *DjYTHDF* are expressed by some neoblasts, as well as *DjYTHDC1* being expressed in the cephalic ganglia, I expected that the loss of these genes would cause evident morphological defects.

Throughout the feeding process, there were no significant changes in morphology after RNAi. This result was confusing as I expected that both readers might have potential roles in neoblasts and cephalic ganglia, as shown in results of figure 2B. To further investigate the effect of depletion of either m⁶A readers, I used RT-qPCR to check the levels of several marker genes for neoblasts as well as neural and eye progeny cells. Using the marker genes for different stages of a neural cell differentiation, I observed that depletion of *DjYTHDC1* resulted in evident changes in expression of almost all cell fractions, with significant changes in expression of *Djtgs-1* (marker gene of cNeoblasts) and *Djsp6-9*. On the other hand, depletion of *DjYTHDF* resulted in a trend towards the

decrease of *Djtgs-1*, increase of *Djap-2* expression as well as decrease in *Djsp6-9* expression (Figure 6).



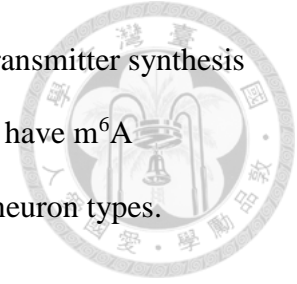
Changes in expression level of cNeoblast marker gene in *DjYTHDC1* or *DjYTHDF* depleted worms could be due to changes in the cell number or change in average expression level in one cell. To test whether the number of cNeoblast was reduced after RNAi, H3P immunofluorescence staining was used to quantify the net number of proliferative cells. The result of this quantification showed evident reduction in the number of proliferative cells in both *DjYTHDC1* and *DjYTHDF* depleted worms (Figure 7B and C). This result indicated that *DjYTHDC1* and *DjYTHDF* play a role in the number of proliferative cells.

3.5. *DjYTHDC1* and *DjYTHDF* are required for expression of neuron subtypes marker genes and regulates planarian behavior

In the previous section, I have shown that m⁶A readers are enriched to the cephalic ganglia and might play a role in the regulation of neural progenitors. To determine whether *DjYTHDC1* and *DjYTHDF* affects the structure of nervous system, I performed WISH for the pan-neuron marker *Djpc-2* in *DjYTHDC1* or *DjYTHDF* depleted worms. However, the WISH results do not show significant changes in the expression pattern of *Djpc-2* (Figure 8A). It is possible that depletion of *DjYTHDC1* or *DjYTHDF* affects a specific neuron type rather than have a general effect on the nervous system. Thus, I further analyzed the different neural subtypes to identify the specific neurons affected by depletion of *DjYTHDC1* and *DjYTHDF*.

Recent studies showed that, m⁶A were linked to the survival of dopaminergic neurons in the brain of mice (Chen et al., 2019). In addition, using the m⁶A modification prediction

tool, REPIC, it was found that the mRNAs of key enzyme in the neurotransmitter synthesis pathway of GABAergic, cholinergic and dopaminergic neurons seem to have m⁶A modification sites. Indicating a possible role of m⁶A readers in various neuron types.



The quantification of expression level showed that depletions of *DjYTHDC1* and *DjYTHDF* seemed to increase the expression of *Djchat* and *Djgad*. Depletion of *DjYTHDC1* and *DjYTHDF* appear to reduce expression of *Djth*, an enzyme expressed in dopaminergic neurons (Figure 8B). WISH of *Djchat* in the *DjYTHDC1*-depleted worms showed that the expression pattern of *Djchat* at the ventral nerve cord seemed to be narrower than that in worm with control YFP RNAi (Figure 8C). WISH of *Djth* in *DjYTHDC1*-depleted worms showed reduced range of *Djth* expression in comparison to control, while *DjYTHDF*-depleted worms appear to have lost the original staining pattern of *Djth* (Figure 8D). Although the expression pattern of *Djgad* was not changed by depletion of *DjYTHDC1* or *DjYTHDF*, the number of cells expressing *Djgad* was significantly increased in *DjYTHDC1*-depleted worms (Figure 8E and F). Taken together, this suggested that in intact worms, *Djchat* and *Djgad* were mainly affected by depletion of *DjYTHDC1* while *Djth* appear to be affected by both *DjYTHDC1* and *DjYTHDF* depletion.

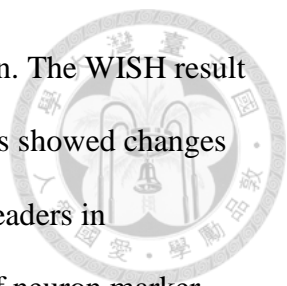
Aside from impacts in gene expression and morphology, m⁶A has also been known to affect behavior of an organism. To analyze the effect of depletion of m⁶A readers on behavior, I used phototaxis assay to evaluate the changes in planarian behavior. Phototaxis assay for planarian was done as illustrated in figure 9A. The planarians were initially located within the dashed line at Q1 zone. The light source is then turned on for 2 minutes, and the worms were expected to move towards Q4. After 2 minutes the light was turned off and the position of the worms were recorded. It can be observed from figure 9B that the

percentage of worms in Q1 is increased in *DjYTHDC1*- and *DjYTHDF*-depleted worms. This indicates that the ability to evade light has been decreased in *DjYTHDC1* and *DjYTHDF* depleted worms, suggesting that *DjYTHDC1* and *DjYTHDF* might regulate the light sensory circuit in planarian.

The decrease in negative phototaxis might indicate defects in the nervous system, photoreceptor cells or the transferring of signal from the photoreceptors to the nervous system. The neuron subtype involved in the negative phototaxis in planarian was the GABAergic neurons, although depletion of *DjYTHDC1* increased the number of *Djgad*⁺ cells, there might be other factors involved in the negative phototaxis response. To further examine this possibility, I performed IF of synapsin and arrestin in *DjYTHDC1* or *DjYTHDF* depleted worms. Staining of Synapsin do not show any evident defects consistent with results from WISH staining of *Djpc-2*. Interestingly, even though the location of optic chiasm did not change following depletion of *DjYTHDC1* and *DjYTHDF* the photoreceptors show slight diffusion in the staining patterns (Figure 9C). This indicates that the reduced negative phototaxis response might be caused by the diffusion of photoreceptors.

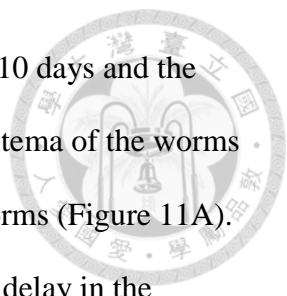
3.6. Depletion of m⁶A readers affects development of several neuron subtypes

Characterization of *DjYTHDC1* and *DjYTHDF* expression in regenerating tissues showed that they are enriched to the newly regenerated brain (Figure 5). In addition, RT-qPCR results have shown that depletion of *DjYTHDC1* and *DjYTHDF* increased the number of neural progeny cells (Figure 6A). This indicates that *DjYTHDC1* and *DjYTHDF*



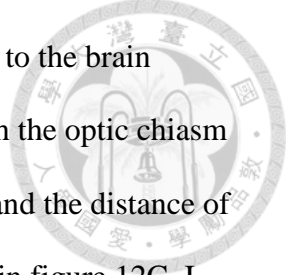
may be highly involved in the process of neural development in planarian. The WISH result of neuron subtype markers in *DjYTHDC1* and *DjYTHDF* depleted worms showed changes in expression pattern. To further characterize the function of both m⁶A readers in development of different neuron subtypes, we analyzed the expression of neuron marker genes for different neuron subtypes in newly regenerated worms. Throughout this study, depletion of *DjYTHDC1* and *DjYTHDF* was done through feeding of dsRNA, however, during regeneration the RNAi treatment has to be stopped because planarians do not eat before the pharynx fully grows back. As a consequence, repression of *DjYTHDC1* and *DjYTHDF* may not be maintained during progression of regeneration. To continue the RNAi effect during regeneration, I applied the method published by (Orii et al., 2003), which demonstrated the effectiveness of soaking regenerating worms in dsRNA to deplete genes in *Dugesia japonica*. The worms were first fed with dsRNA twice a week for 4 weeks, after that they were amputated and soaked in dsRNA twice every week for 2 weeks. After 2 weeks, the worms were fixed in Trizol and the total RNA were collected, followed by RT-qPCR to check for the levels of *DjYTHDC1* and *DjYTHDF* after dsRNA soaking (Figure 10A). The anterior regenerating tissue of each worm was used as the control. Figure 10B and 10C showed that after soaking treatment, the level of *DjYTHDC1* and *DjYTHDF* were maintained at a low level at the end of the 14-day regeneration. This proves that soaking is an effective method to deplete expression level of *DjYTHDC1* and *DjYTHDF* in regenerating worms.

After confirming that the soaking method was effective in repressing the expression of *DjYTHDC1* and *DjYTHDF*, I performed amputation of worms that had undergone RNAi of *DjYTHDC1* and *DjYTHDF*. After feeding for 8 turns, the worms were starved for 4 days



before it is cut into 3 sections. Each section was observed separately for 10 days and the status of regeneration were recorded (Figure 10A). I noticed that the blastema of the worms with *DjYTHDC1* RNAi were smaller in size in comparison to control worms (Figure 11A). In addition, the anterior blastema of the mid-piece and tail showed some delay in the regeneration of new eyes (Figure 11B). All control worms were able to regenerate both eyes within 6 days post-amputation, however most *DjYTHDC1* and *DjYTHDF* RNAi worms regenerate both eyes at 9 days post amputation. In addition, the rate of regeneration for both eyes were the same in all control worms. However, RNAi worms showed different rates of regeneration in each eye, leading to the appearance of intermediary phenotypes in the worms such as one-eyed or asymmetrical eye phenotypes during regeneration before eventually regenerating both eyecups. Some RNAi worms were more severe in the sense that it was not able to regenerate symmetrical eyecups, and worms with asymmetrical eyespots were still present at the last day of observation.

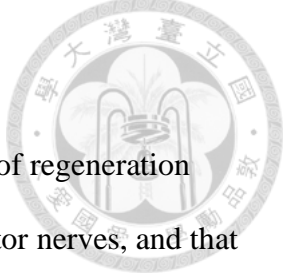
The delay of eyespot formation could be caused by various factors such as delay in pigment formation, optic chiasm formation, pole formation, and many more. To elucidate the cause of eyespot formation delay, I performed the double IF with antibodies against synapsin and arrestin in the regenerating worms. At both 4- and 7-days post amputation, the staining results indicated that the overall morphology of the nervous system was not affected. The position of eyespots was in the anterior indicating that the anterior – posterior pole formation was not disrupted. At both 4- and 7- days after amputation, the optic chiasma was formed in *DjYTHDC1* and *DjYTHDF* depleted worms, however, there was abnormality in the overall shape of the optic nerves (Figure 12A and B). Normally, the nerves of photoreceptor cells first bundle together and extend from each eyespot to form the



optic chiasm. The nerves then elongate downwards to form a connection to the brain (Scimone et al., 2020). The nerve connecting the photoreceptor cells with the optic chiasm seemed to be shorter in comparison to control. The length of the nerves and the distance of two eyes were used for the quantification of eye nerve length as defined in figure 12C. I found that the length of eye nerve in *DjYTHDC1* and *DjYTHDF* depleted worms at day 4 and day 7 were significantly shorter than control worms (Figure 12D). This result suggested that the delay in eyespot formation may be due to delay in the elongation of nerve between photoreceptor and optic chiasma.

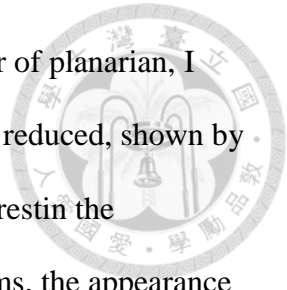
We next tested whether m⁶A readers will affect the differentiation of various neuron subtypes. The normal expression pattern of *Djgad* is a U-shaped expression in the area around the two eyespots (Figure 13A). However, in both *DjYTHDC1* and *DjYTHDF* there seems to be aberrant expression of *Djgad*. Expression of *Djgad* in *DjYTHDC1*-depleted worms appear to have a concentrated expression in between the 2 eyespots, and *DjYTHDF* depleted worms appear to have narrowed expression of *Djgad* near the eyespots (Figure 13B). The result of *Djth* staining showed that the pattern of expression was changed in *DjYTHDC1*- or *DjYTHDF*-depleted worms. The normal expression pattern of *Djth* is a straight line underneath the eyespots and they are generally quite symmetrical. However, in *DjYTHDC1*- and *DjYTHDF*-depleted worms it seemed that the *Djth* pattern became asymmetrical and abnormal in shape (Figure 13C). Results of *Djchat* WISH suggested that the level of *Djchat* was greatly reduced in *DjYTHDF*-depleted worms, in comparison to both control and *DjYTHDC1* depleted worms. In contrast, *DjYTHDC1* depleted worms seem to have an increased expression of *Djchat* (Figure 13D).

4. Discussion



In this study I found that *DjYTHDF* is important in the later stages of regeneration such as positioning of the optic chiasm and elongation of the photoreceptor nerves, and that *DjYTHDC1* may be important in the maintenance of proliferative cells and earlier stages of regeneration. It would be interesting to further elucidate the mechanisms by which the m⁶A readers affect cell differentiation and turnover. To do this, I will try to identify the target RNAs that are regulated by binding of the m⁶A readers to the m⁶A mark. A method called RNA-CLIP-Seq will be considered for this aim. By treating the planarian lysate with UV cross-linking, the covalent bonds between the reader proteins and their RNAs will strengthen the interacting complex. Then using the anti- *DjYTHDC1* antibody I will precipitate the complex, followed by the RNA extraction. I could use NGS to obtain the sequences of the target RNAs or use RT-qPCR to check for the presence of candidate genes. Some candidate genes, including several well-researched targets of m⁶A readers such as *not1*, *SRSF3* and many more, will be present in the RIP-Seq results. After identifying the target RNAs, I would perform WISH and possibly use FISH to further analyze the interaction of the readers with the targeted RNAs, as well as understand the downstream mechanism of *DjYTHDC1* and *DjYTHDF* in regulating planarian homeostasis and regeneration.

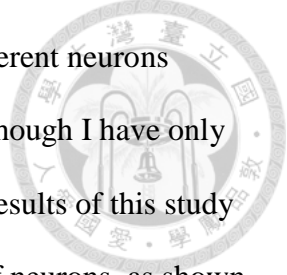
Through WISH analysis for marker genes of specific neural subtypes, I observed the reduction in expression in both cholinergic and dopaminergic neurons after *DjYTHDC1* and *DjYTHDF* depletion (Figure 8B-D). As the marker genes I have selected are enzymes responsible for the synthesis of the specific neurotransmitters, I also examined if the reduced expression of these enzymes would affect the function of these neurons by testing



the behavior of planarian. Through quantification of phototactic behavior of planarian, I found that the ability of m⁶A reader - depleted worms to evade light was reduced, shown by the high proportion of worms in Q1 (Figure 9B). Through staining of Arrestin the photoreceptor cells appear to be more diffused compared to control worms, the appearance of diffused photoreceptor cells might indicate a less compact organization of nerves. The disorganization of the photoreceptor cells could contribute to the reduction of negative phototaxis behavior, although more investigation is needed to prove this hypothesis. Negative phototaxis was found to be regulated by GABAergic neurons in planarian although to my knowledge the detailed analysis of its mechanism has not been studied. In addition, phototactic behavior of planarian also requires coordinated muscle movement as well as the sensing of light. Therefore, to further examine the effect of m⁶A modification on behavior, a combination of different behavioral tests or neurobiology methods may be needed.

Further characterization of the role of m⁶A readers in development was done through analysis of m⁶A reader expression in regeneration. Double IF of Synapsin and Arrestin showed the shortened nerve from the photoreceptor cells towards the optic chiasm. It appears that the depletion of *DjYTHDC1* and *DjYTHDF* altered the mechanisms that ensure proper positioning of the optic nerves. We also discovered that depletion of m⁶A readers caused the increased expression of *Djchat* in newly regenerated worms, while the expression of *Djth* became asymmetric. Depletion of *DjYTHDC1* and *DjYTHDF* also causes aberrant expression pattern of *Djgad*.

Function of neurons are interrelated in the sensory system, and behavior of an organism are often a result of the interaction between several different groups of neurons.



In the case of regeneration, the establishment of interaction between different neurons might determine the rate of functional recovery in neuronal systems. Although I have only explored the morphological recovery of the neurons after regeneration, results of this study have also shown that m⁶A reader depletions are able to affect function of neurons, as shown by phototaxis assay in intact worms. Therefore, it is also possible that depletion of m⁶A readers will also affect the rate of functional recovery of neurons, however, due to time limitations I was not able to test this hypothesis yet.

The altered symmetry of *Djth* as well as the ectopic expression of *Djgad* in RNAi worms seem to indicate a possible role of both m⁶A readers in recovery of polarity in the newly regenerated neurons. It has been shown that the TALE-homeobox gene *pbx* was expressed in the cephalic ganglia and participated in the formation and maintenance of anterior-posterior poles as well as eye progenitor (Chen et al., 2013). In addition, analysis of the gene in mammalian m⁶A database REPIC shows that it is indeed m⁶A-modified. This suggests a possible mechanism of pole formation by which *pbx* interacts with m⁶A readers to determine the expression pattern of neurons.

In summary, the results presented in this study revealed that m⁶A readers are heavily involved in the development of neurons. m⁶A readers can function at three aspects involved in regeneration and neuron development: First, the proliferation of neoblasts and neuron precursor cells; second, the differentiation of neoblasts and neuron precursor cells; and third, the maintenance of balance between cell death and cell proliferation. Further analysis of the effect of long-term m⁶A reader depletion on neurons will help us to pinpoint the mechanism by which m⁶A readers affect planarian regeneration and neuron development.

5. References



- Chen, C.C., Wang, I.E., and Reddien, P.W. (2013). *pbx* is required for pole and eye regeneration in planarians. *Development* *140*, 719-729. 10.1242/dev.083741.
- Chen, X., Yu, C., Guo, M., Zheng, X., Ali, S., Huang, H., Zhang, L., Wang, S., Huang, Y., Qie, S., and Wang, J. (2019). Down-Regulation of m6A mRNA Methylation Is Involved in Dopaminergic Neuronal Death. *ACS Chem Neurosci* *10*, 2355-2363. 10.1021/acscemneuro.8b00657.
- Forsthoefel, D.J., Ross, K.G., Newmark, P.A., and Zayas, R.M. (2018). Fixation, Processing, and Immunofluorescent Labeling of Whole Mount Planarians. *Methods Mol Biol* *1774*, 353-366. 10.1007/978-1-4939-7802-1_10.
- Kan, L., Ott, S., Joseph, B., Park, E.S., Dai, W., Kleiner, R.E., Claridge-Chang, A., and Lai, E.C. (2021). A neural m(6)A/Ythdf pathway is required for learning and memory in *Drosophila*. *Nat Commun* *12*, 1458. 10.1038/s41467-021-21537-1.
- Lence, T., Akhtar, J., Bayer, M., Schmid, K., Spindler, L., Ho, C.H., Kreim, N., Andrade-Navarro, M.A., Poeck, B., Helm, M., and Roignant, J.-Y. (2016). m6A modulates neuronal functions and sex determination in *Drosophila*. *Nature* *540*, 242-247. 10.1038/nature20568.
- Lence, T., Soller, M., and Roignant, J.-Y. (2017). A fly view on the roles and mechanisms of the m(6)A mRNA modification and its players. *RNA Biol* *14*, 1232-1240. 10.1080/15476286.2017.1307484.
- Lewis, C.J., Pan, T., and Kalsotra, A. (2017). RNA modifications and structures cooperate to guide RNA-protein interactions. *Nat Rev Mol Cell Biol* *18*, 202-210. 10.1038/nrm.2016.163.
- Li, A., Chen, Y.-S., Ping, X.-L., Yang, X., Xiao, W., Yang, Y., Sun, H.-Y., Zhu, Q., Baidya, P., Wang, X., et al. (2017). Cytoplasmic m6A reader YTHDF3 promotes mRNA translation. *Cell Res* *27*, 444-447. 10.1038/cr.2017.10.
- Li, M., Zhao, X., Wang, W., Shi, H., Pan, Q., Lu, Z., Perez, S.P., Suganthan, R., He, C., Bjørås, M., and Klungland, A. (2018). Ythdf2-mediated m(6)A mRNA clearance modulates neural development in mice. *Genome Biol* *19*, 69. 10.1186/s13059-018-1436-y.
- Liu, C., Cao, J., Zhang, H., and Yin, J. (2022). Evolutionary History of RNA Modifications at N6-Adenosine Originating from the R-M System in Eukaryotes and Prokaryotes. *Biology* *11*, 214. 10.3390/biology11020214.
- Liu, J., and Jia, G. (2014). Methylation modifications in eukaryotic messenger RNA. *J Genet Genomics* *41*, 21-33. 10.1016/j.jgg.2013.10.002.

Meyer, K.D., Patil, D.P., Zhou, J., Zinoviev, A., Skabkin, M.A., Elemento, O., Pestova, T.V., Qian, S.-B., and Jaffrey, S.R. (2015). 5' UTR m(6)A Promotes Cap-Independent Translation. *Cell* 163, 999-1010. 10.1016/j.cell.2015.10.012.

Nishikura, K. (2016). A-to-I editing of coding and non-coding RNAs by ADARs. *Nat Rev Mol Cell Biol* 17, 83-96. 10.1038/nrm.2015.4.

Orii, H., Mochii, M., and Watanabe, K. (2003). A simple "soaking method" for RNA interference in the planarian *Dugesia japonica*. *Dev Genes Evol* 213, 138-141. 10.1007/s00427-003-0310-3.

Paskin, T.R., Jellies, J., Bacher, J., and Beane, W.S. (2014). Planarian Phototactic Assay Reveals Differential Behavioral Responses Based on Wavelength. *PLoS One* 9, e114708. 10.1371/journal.pone.0114708.

Patil, D.P., Pickering, B.F., and Jaffrey, S.R. (2018). Reading m(6)A in the Transcriptome: m(6)A-Binding Proteins. *Trends Cell Biol* 28, 113-127. 10.1016/j.tcb.2017.10.001.

Pearson, B.J., Eisenhoffer, G.T., Gurley, K.A., Rink, J.C., Miller, D.E., and Sánchez Alvarado, A. (2009). Formaldehyde-based whole-mount in situ hybridization method for planarians. *Dev Dyn* 238, 443-450. 10.1002/dvdy.21849.

Rink, J.C. (2013). Stem cell systems and regeneration in planaria. *Dev Genes Evol* 223, 67-84. 10.1007/s00427-012-0426-4.

Roscito, J.G., Sameith, K., Parra, G., Langer, B.E., Petzold, A., Moebius, C., Bickle, M., Rodrigues, M.T., and Hiller, M. (2018). Phenotype loss is associated with widespread divergence of the gene regulatory landscape in evolution. *Nat Commun* 9, 4737. 10.1038/s41467-018-07122-z.

Ross, K.G., Currie, K.W., Pearson, B.J., and Zayas, R.M. (2017). Nervous system development and regeneration in freshwater planarians. *Wiley Interdiscip Rev Dev Biol* 6. 10.1002/wdev.266.

Roundtree, I.A., Luo, G.-Z., Zhang, Z., Wang, X., Zhou, T., Cui, Y., Sha, J., Huang, X., Guerrero, L., Xie, P., et al. (2017). YTHDC1 mediates nuclear export of N(6)-methyladenosine methylated mRNAs. *Elife* 6, e31311. 10.7554/eLife.31311.

Scimone, M.L., Atabay Kutay, D., Fincher Christopher, T., Bonneau Ashley, R., Li Dayan, J., and Reddien Peter, W. (2020). Muscle and neuronal guidepost-like cells facilitate planarian visual system regeneration. *Science* 368, eaba3203. 10.1126/science.aba3203.

Shi, H., Wang, X., Lu, Z., Zhao, B.S., Ma, H., Hsu, P.J., Liu, C., and He, C. (2017). YTHDF3 facilitates translation and decay of N6-methyladenosine-modified RNA. *Cell Res* 27, 315-328. 10.1038/cr.2017.15.

Wang, X., Zhao, B.S., Roundtree, I.A., Lu, Z., Han, D., Ma, H., Weng, X., Chen, K., Shi, H., and He, C. (2015). N(6)-methyladenosine Modulates Messenger RNA Translation Efficiency. *Cell* 161, 1388-1399. 10.1016/j.cell.2015.05.014.

Zeng, A., Li, H., Guo, L., Gao, X., McKinney, S., Wang, Y., Yu, Z., Park, J., Semerad, C., Ross, E., et al. (2018). Prospectively Isolated Tetraspanin(+) Neoblasts Are Adult Pluripotent Stem Cells Underlying Planaria Regeneration. *Cell* 173, 1593-1608.e1520. 10.1016/j.cell.2018.05.006.

Zhao, B.S., Wang, X., Beadell, A.V., Lu, Z., Shi, H., Kuuspalu, A., Ho, R.K., and He, C. (2017). m6A-dependent maternal mRNA clearance facilitates zebrafish maternal-to-zygotic transition. *Nature* 542, 475-478. 10.1038/nature21355.

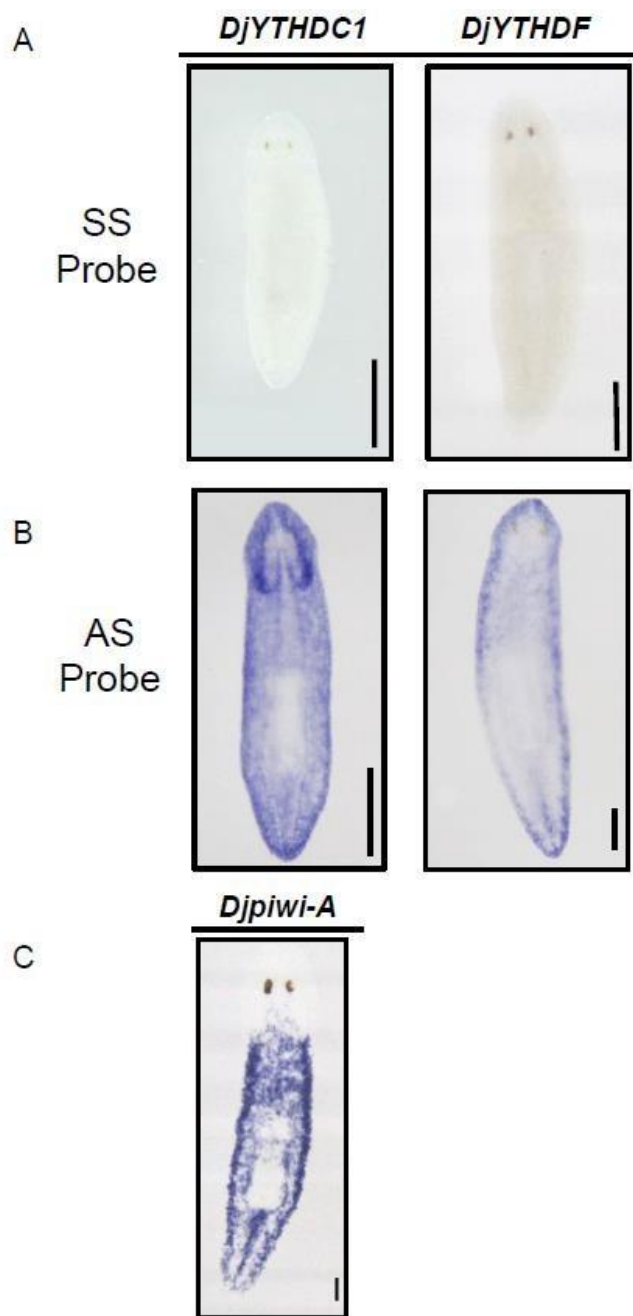


Figure 2. Expression of *DjYTHDC1* and *DjYTHDF* in planarian. Wholemount in situ hybridization (WISH) of m⁶A readers in intact planarian showed that *DjYTHDC1* was highly expressed in the cephalic ganglia of the worm with some expression in the parenchyma. While *DjYTHDF* is expressed diffused throughout the parenchyma. (Scale bar =500μm)

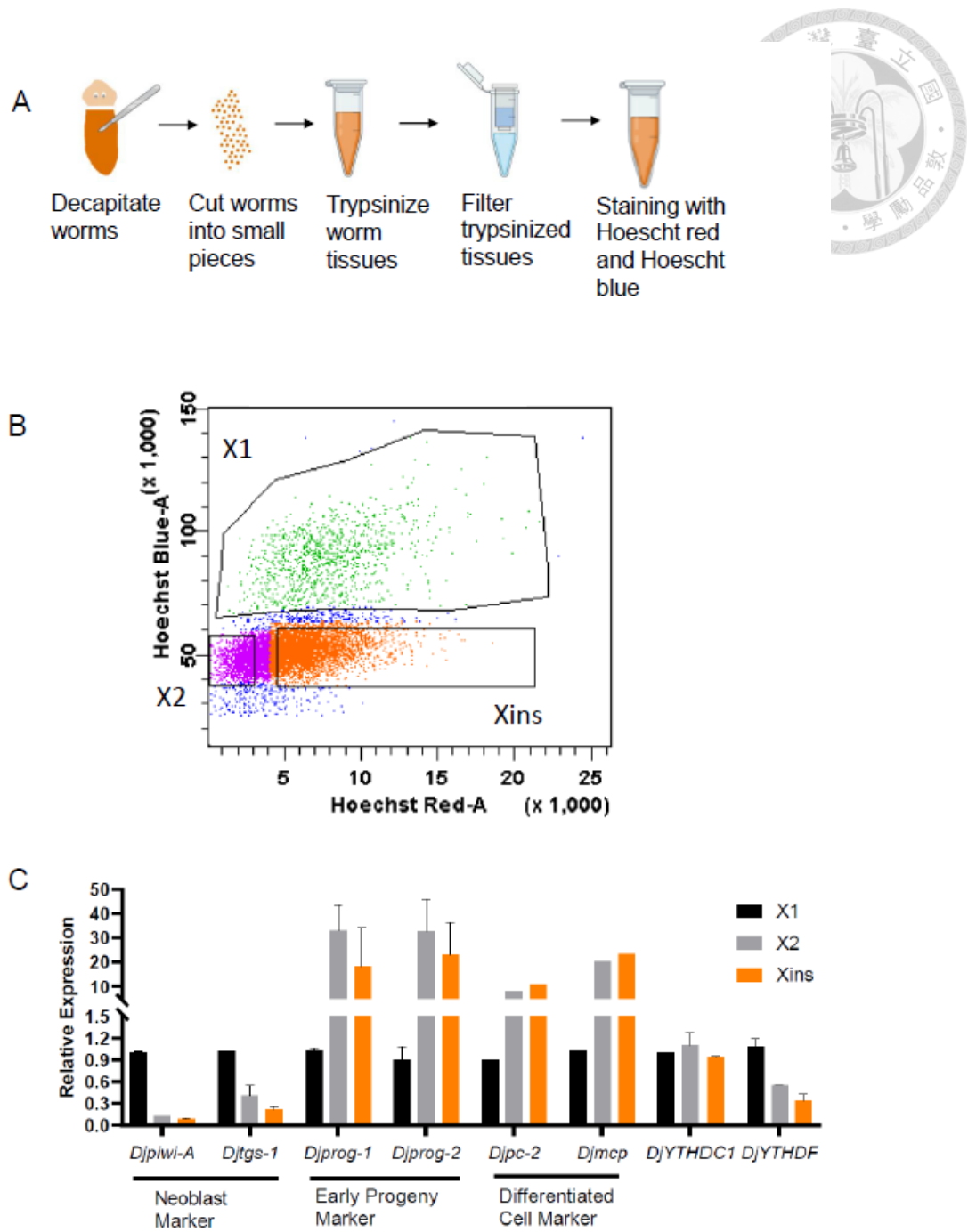


Figure 3. The expression of m⁶A readers in various groups of planarian cells isolated by FACS. (A) Work flow of isolating planarian cells by FACS. (B) Gating of X1, X2, and Xins using Hoescht red (cell size) and Hoescht blue (DNA content) fluorescence. (C) RT-qPCR analysis for the mRNA levels of m⁶A readers and cell type marker genes in X1, X2, Xins cells from decapitated worms (n = 2).

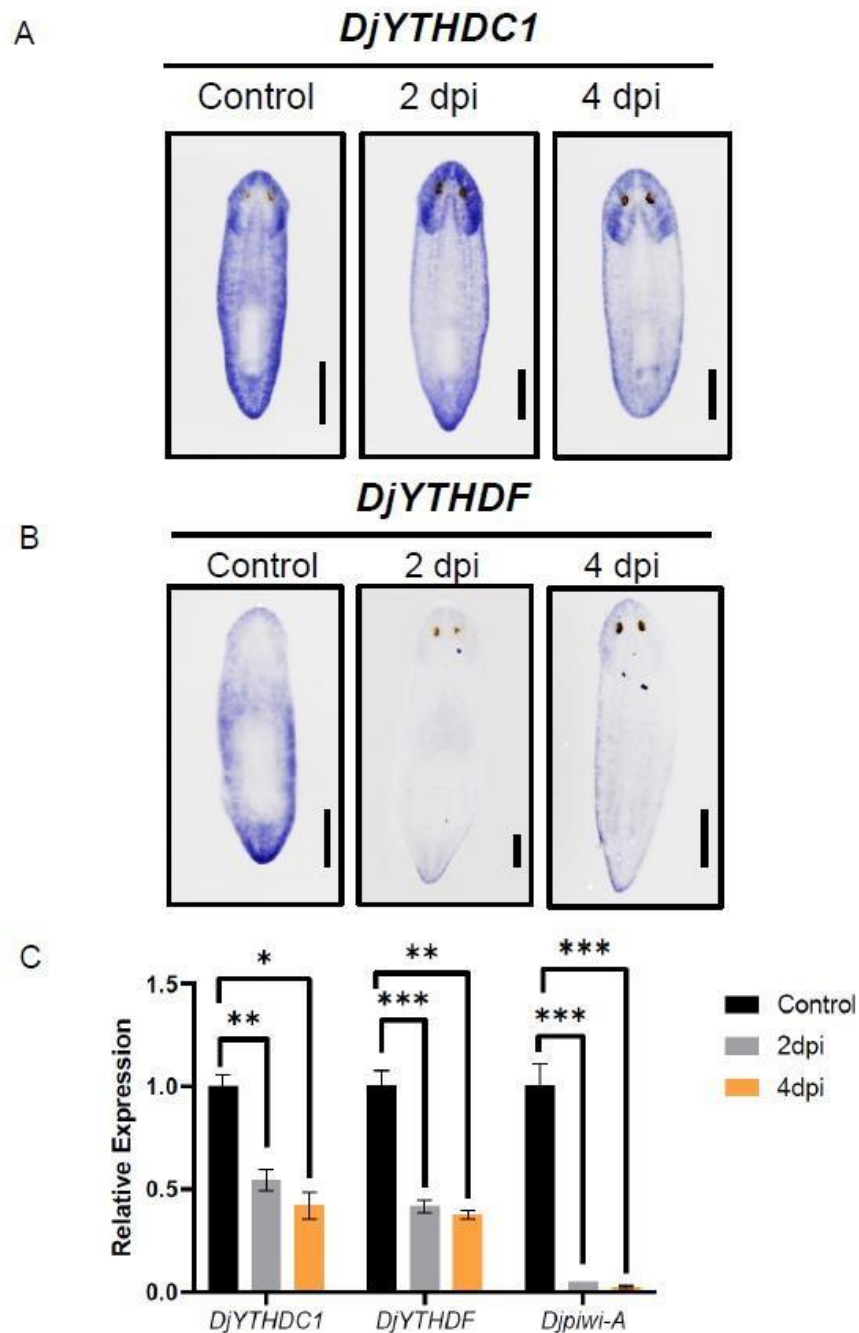


Figure 4. The expression of *DjYTHDC1* and *DjYTHDF* were reduced in planarian after γ -irradiation. WISH of (A) *DjYTHDC1* and (B) *DjYTHDF* in irradiated worms on day 2 and 4 after irradiation (dpi, days after irradiation). The neoblast-like distribution of *DjYTHDC1* and *DjYTHDF* in parenchymal tissues are significantly reduced. (Scale bar = 500 μ m) (C) RT-qPCR quantification of *DjYTHDC1* and *DjYTHDF* in irradiated worms, with *Djpiwi-A* as the neoblast marker showing the elimination of neoblasts after irradiation. Statistical analysis was done using two-tailed student t-test. (error bar = Standard deviation, * = $p < 0.05$, ** = $p < 0.01$, *** = $p < 0.001$)

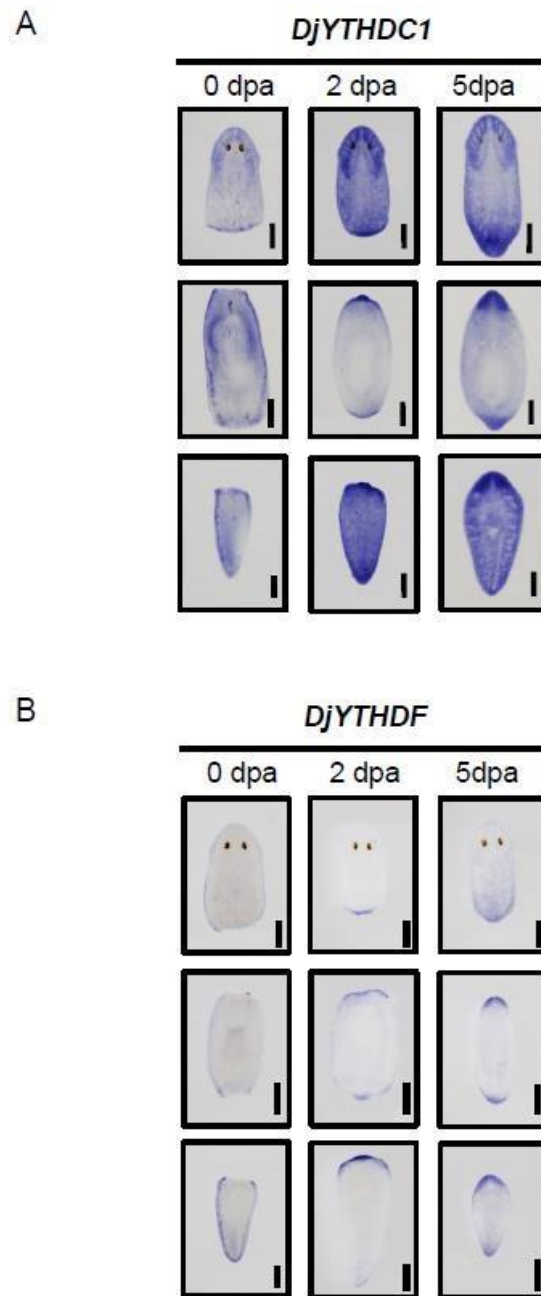


Figure 5. m⁶A readers were highly expressed in the blastema of regenerating planarian. (A) Whole mount in situ hybridization (WISH) for *DjYTHDC1* in regenerating planarian. (B) WISH for *DjYTHDF* in regenerating planarian. (dpa, days after amputation, Scale bar =500μm)

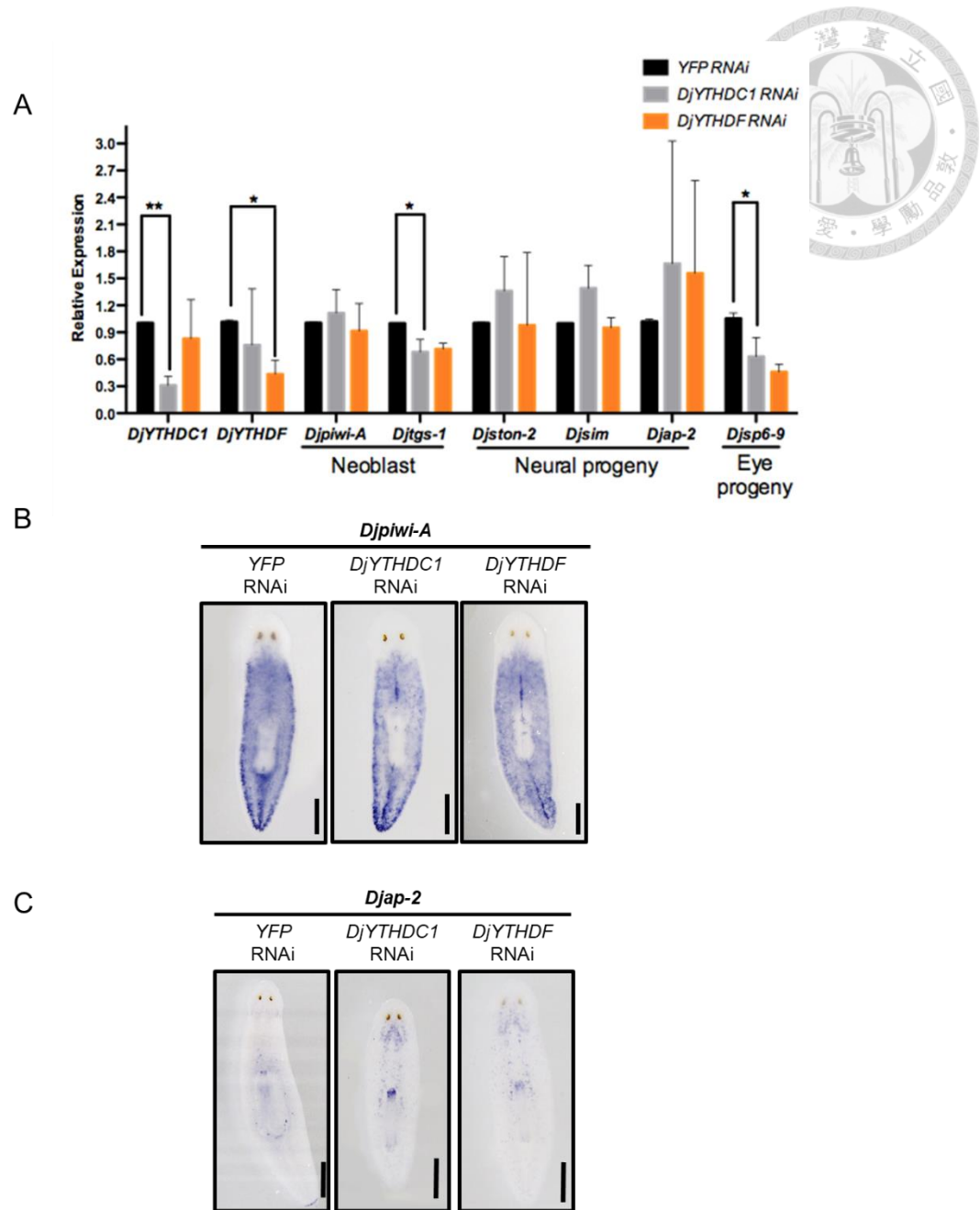
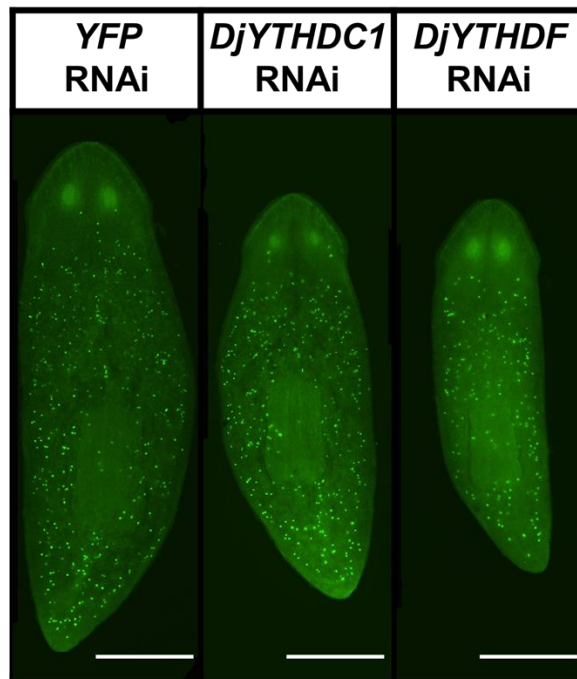


Figure 6. Characterization of *DjYTHDC1* and *DjYTHDF* function in neoblast and progeny cells. (A) RT-qPCR quantification of RNAi effect on the level of marker genes for various cell types. Statistical analysis was done using two-tailed student t-test (error bar = Standard deviation, * = $p < 0.05$, ** = $p \leq 0.01$, *** = $p \leq 0.001$). WISH of (B) *Djpiwi-A*; (C) *Djap-2*, in *DjYTHDC1* or *DjYTHDF* RNAi worms (Scale bar=500 μ m).



A



B

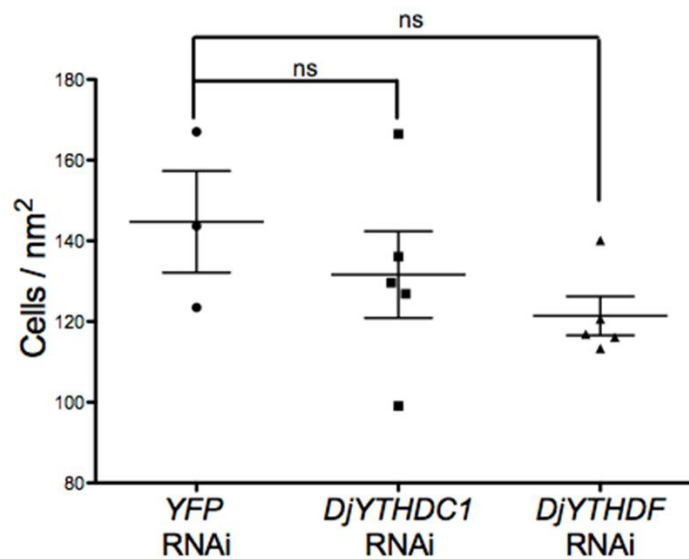


Figure 7. Analysis of the effects of m⁶A reader RNAi on proliferative cells. (A) H3P immunostaining of *DjYTHDC1* and *DjYTHDF* depleted worms (Scale bar = 200 μ m). (B) Quantification of H3P⁺ cell. Statistical analysis was done using two-tailed student t-test. (error bar = Standard deviation, * = $p < 0.05$, ** = $p \leq 0.01$, *** = $p \leq 0.001$)

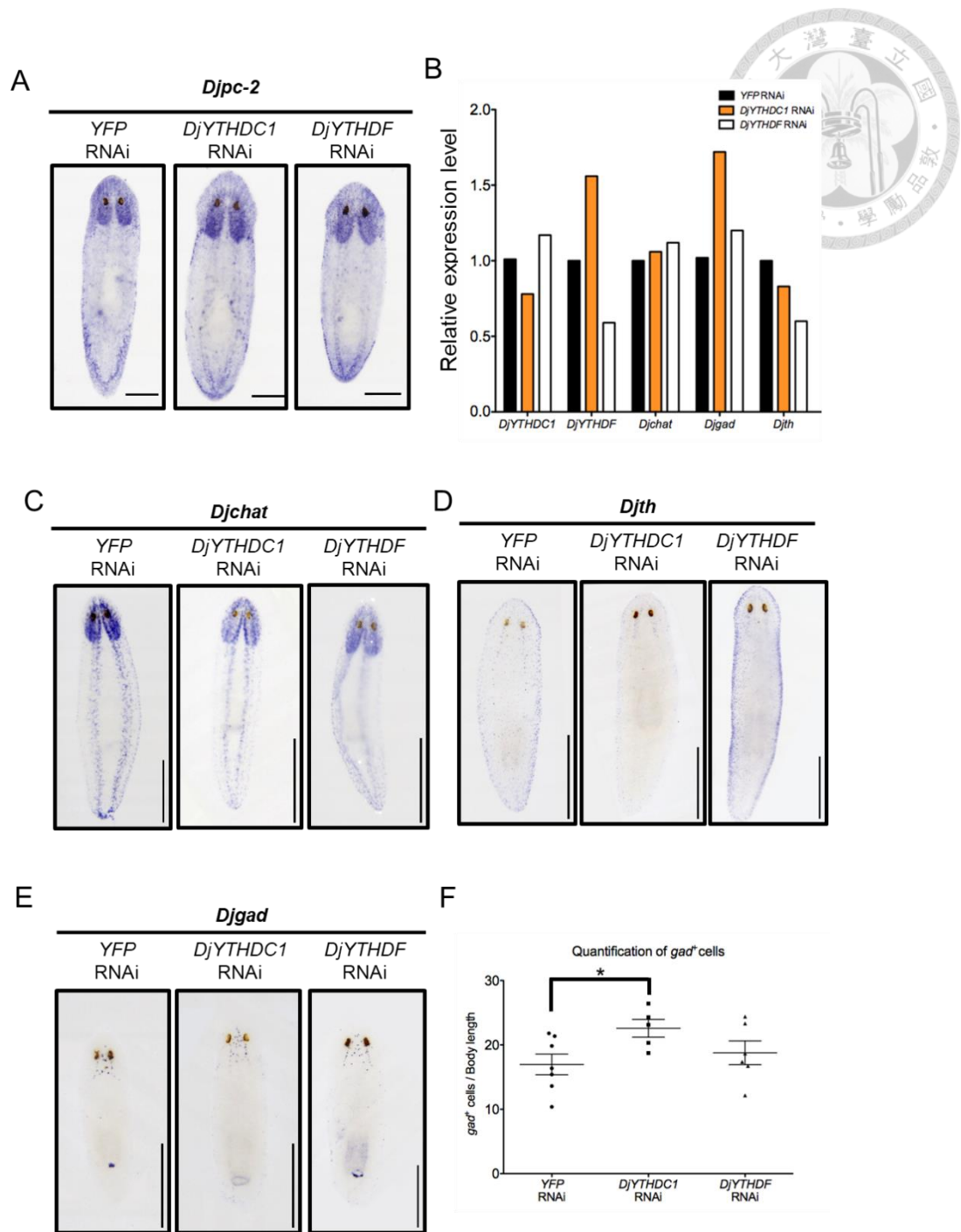


Figure 8. Characterization of *DjYTHDC1* and *DjYTHDF* functions in neuronal system (A) WISH of *Djpc-2* in RNAi worms; WISH of (B) cholinergic neurons using *Djchat* as marker gene; (C) dopaminergic neurons using *Djth* as marker gene (D) GABAergic neurons using *Djgad* as marker gene. (E) Quantification of *Djgad*⁺ cells in *DjYTHDC1*- or *DjYTHDF*-depleted worms.

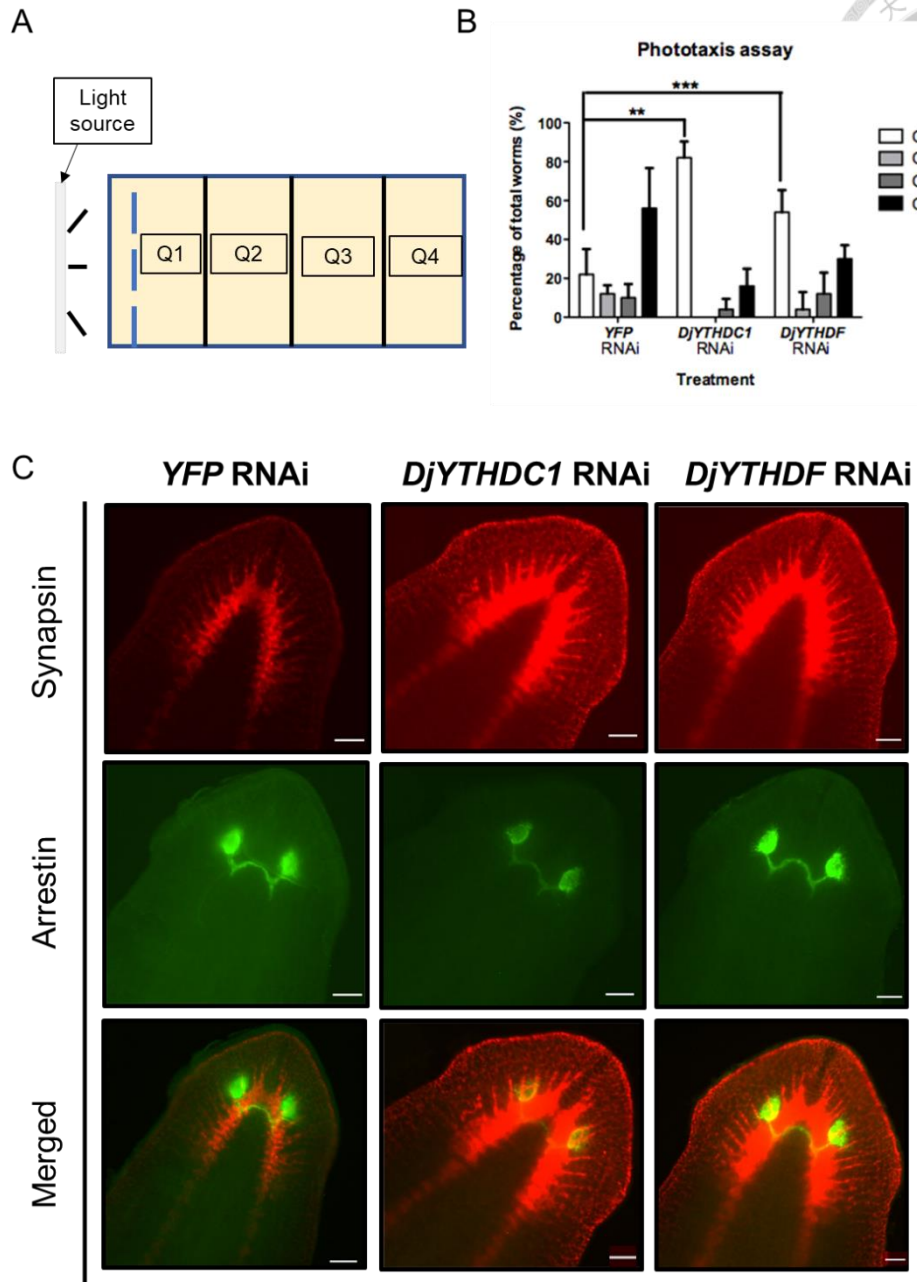
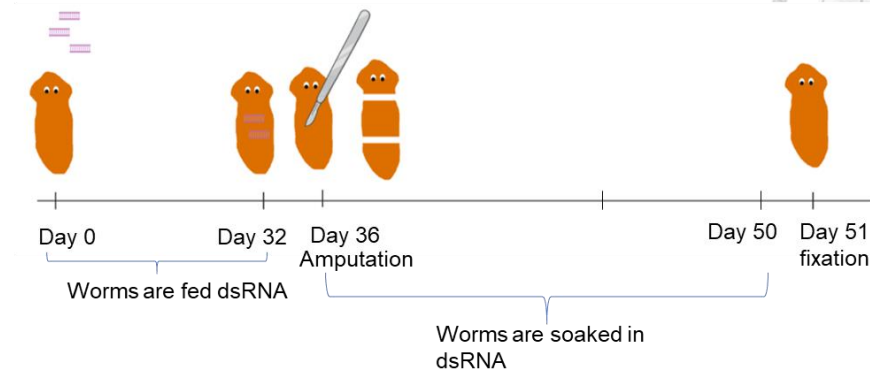
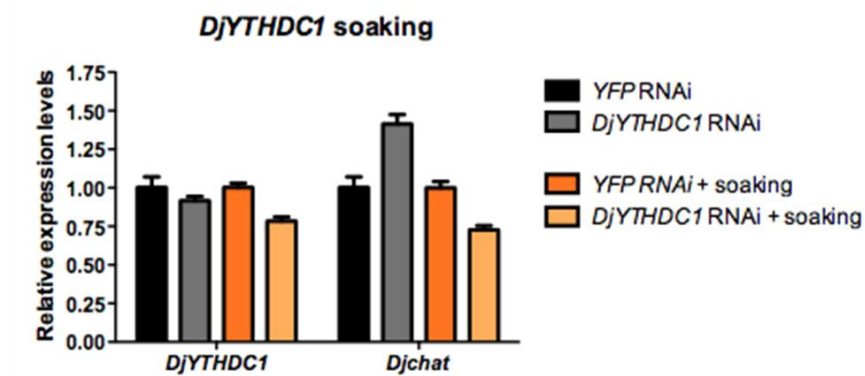


Figure 9. Depletion of *DjYTHDC1* and *DjYTHDF* reduced the negative phototaxis of planarian behavior (A) An illustration of experiment design for phototaxis assay (B) Quantification of phototaxis assay results. Statistical analysis was done using two-tailed student t-test of the percentage of worms in Q1. (error bar = Standard deviation, * = $p < 0.05$, ** = $p \leq 0.01$, *** = $p \leq 0.001$) (C) Immunostaining of Synapsin and Arrestin in *DjYTHDC1* and *DjYTHDF* depleted worms. (Scale bar = 100 μ m)

A



B



C

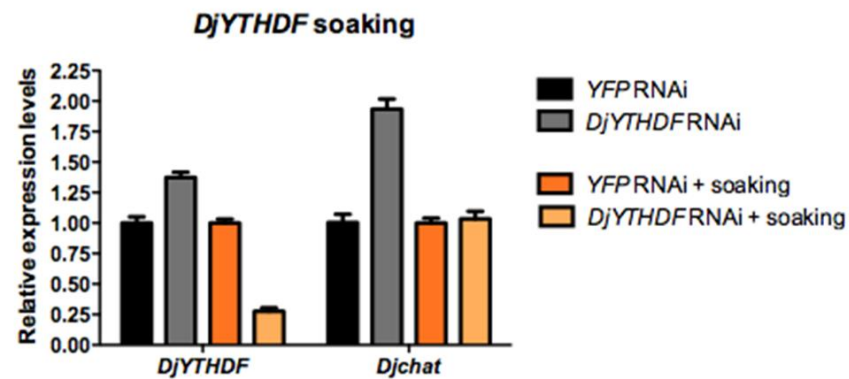
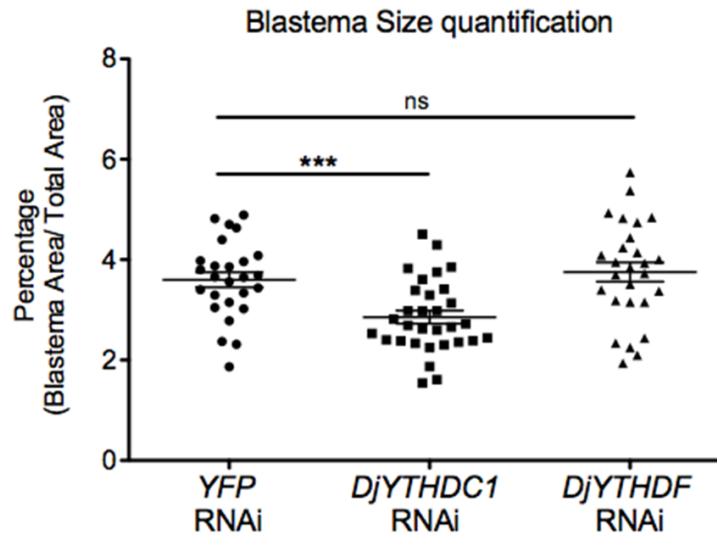


Figure 10. RNAi by soaking in regenerating planarian showed the increased RNAi efficiency (A) Timeline of RNAi (B) RT-qPCR analysis of *DjYTHDF* expression level in control and soaked worms shows low level of *DjYTHDF* in soaked worms (C) RT-qPCR analysis of *DjYTHDC1* expression level in control and soaked worms shows low levels of *DjYTHDC1* in soaked worms



A



B

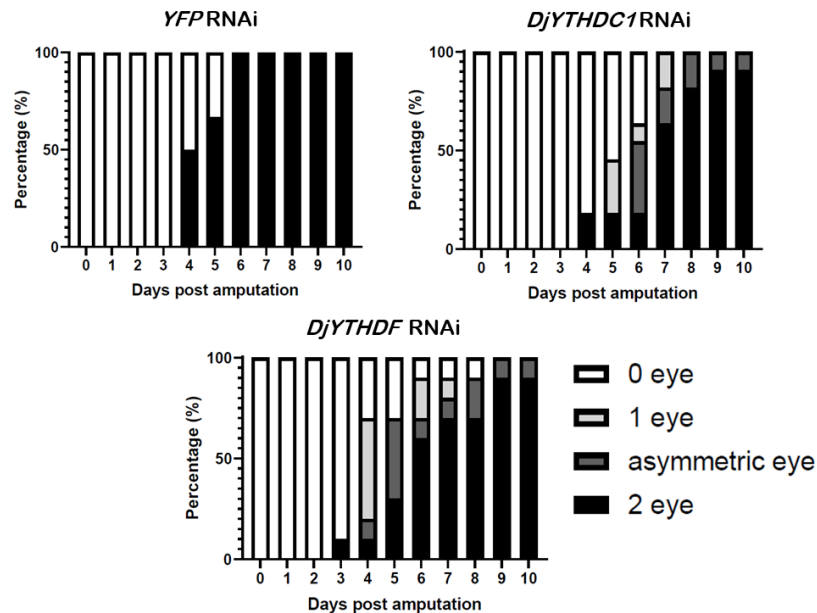


Figure 11. Characterization of the function of m⁶A readers in planarian regeneration.

(A) Quantification of blastema size at 3 dpa during planarian regeneration in control and RNAi worms. Statistical analysis was done using two-tailed student t-test. (error bar = Standard deviation, * = $p < 0.05$, ** = $p \leq 0.01$, *** = $p \leq 0.001$) (B) Depletion of m⁶A readers slightly delayed the eye regeneration.

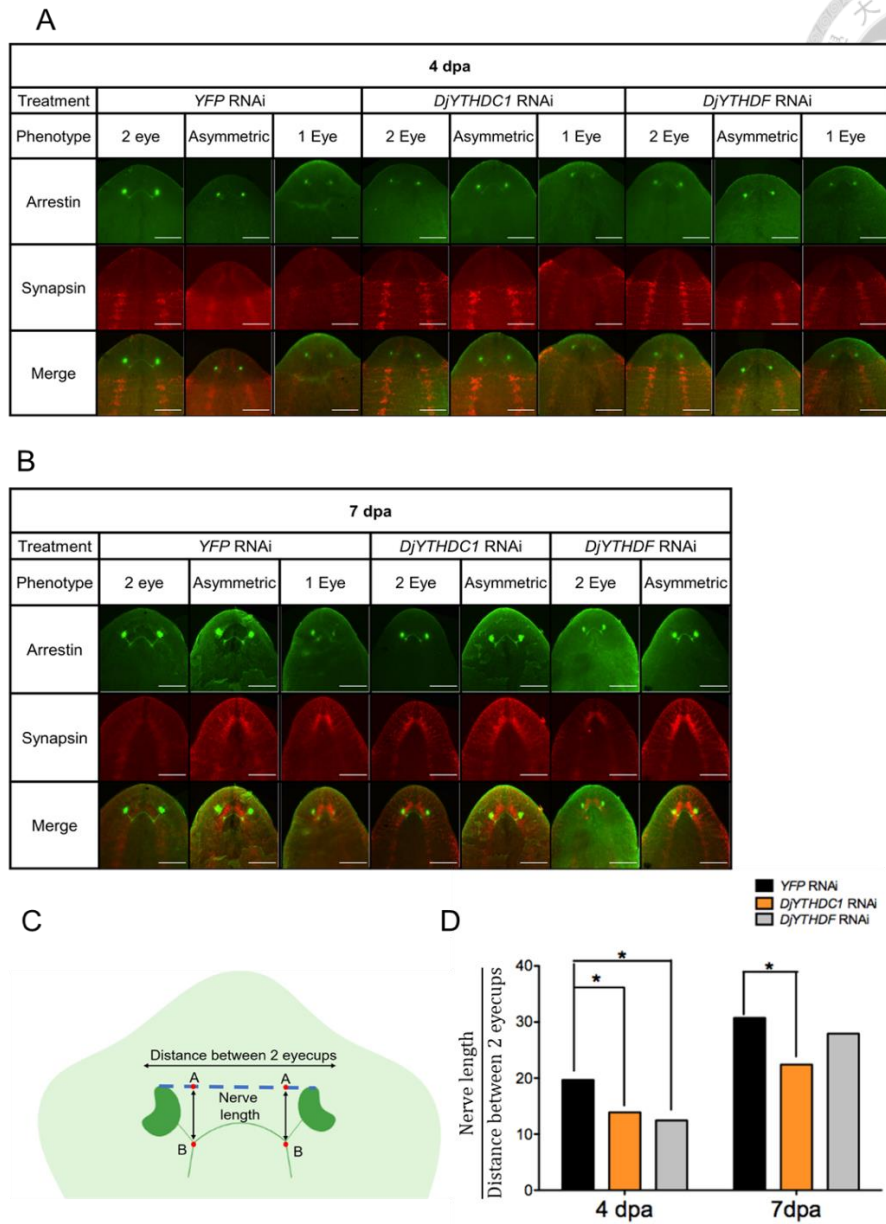


Figure 12. Depletion of m⁶A readers delayed the eye and neuronal regeneration in planarian. The eye and neuronal regeneration processes were detected by immunostaining with arrestin and synapsin at (A) 4 dpa and (B) 7 dpa. (dpa = days post amputation, Scale Bar = 200 μ m) (C) Schematic illustrating the definition of two factors utilized to quantify the length of optical nerves. Point B was the intersection of nerve from photoreceptor and the optic chiasm. A vertical line from B was perpendicular to the connecting line of two eyecups at point A, the optical nerve length was defined as the distance between A and B. (D) Quantification of optical nerve length in worms that regenerated both eyecups. Statistical analysis was done using two-tailed student t-test of the average between left and right nerve. (error bar = Standard deviation, * = $p < 0.05$, ** = $p \leq 0.01$, *** = $p \leq 0.001$)

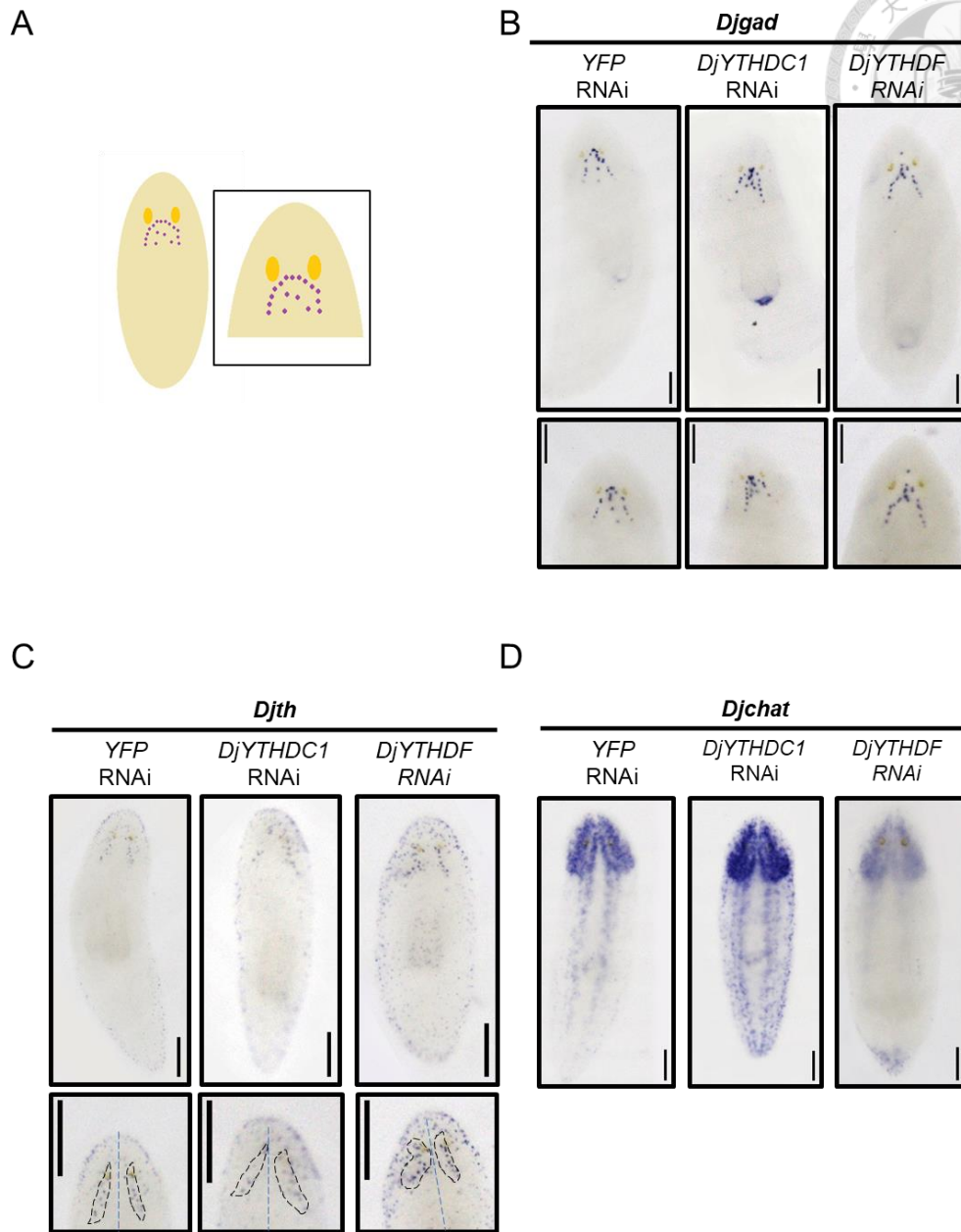


Figure 13. Analysis of the effect of *DjYTHDF* and *DjYTHDC1* depletion in development and differentiation of various types of neurons. (A) A representation of normal *Djgad* staining in intact worm and WISH of (B) *Djgad* (C) *Djchat* (D) *Djth* in 14 dpa worms (dpa = days post amputation; Scale bar=100μm)